

RSC Advances



This is an *Accepted Manuscript*, which has been through the Royal Society of Chemistry peer review process and has been accepted for publication.

Accepted Manuscripts are published online shortly after acceptance, before technical editing, formatting and proof reading. Using this free service, authors can make their results available to the community, in citable form, before we publish the edited article. This *Accepted Manuscript* will be replaced by the edited, formatted and paginated article as soon as this is available.

You can find more information about *Accepted Manuscripts* in the [Information for Authors](#).

Please note that technical editing may introduce minor changes to the text and/or graphics, which may alter content. The journal's standard [Terms & Conditions](#) and the [Ethical guidelines](#) still apply. In no event shall the Royal Society of Chemistry be held responsible for any errors or omissions in this *Accepted Manuscript* or any consequences arising from the use of any information it contains.

ARTICLE

Role of carbon content in qualifying $\text{Li}_3\text{V}_2(\text{PO}_4)_3/\text{C}$ as a high capacity anode for high rate lithium battery applications

V. Mani, K. Nathiya and N. Kalaiselvi*

Cite this: DOI: 10.1039/x0xx00000x

Received 00th January 2012,
Accepted 00th January 2012

DOI: 10.1039/x0xx00000x

www.rsc.org/

Nanocrystalline $\text{Li}_3\text{V}_2(\text{PO}_4)_3$ has been prepared by oxalic dihydrazide assisted combustion (ODHAC) method and the corresponding $\text{Li}_3\text{V}_2(\text{PO}_4)_3/\text{C}$ composites containing different concentration of super P carbon, viz. 10, 20 and 30 wt.% have been explored individually as anode for lithium batteries. Among the chosen composites, $\text{Li}_3\text{V}_2(\text{PO}_4)_3/\text{C}-20$ exhibits superior electrochemical properties, thus recommending a carbon content of 20 wt.% as an optimum amount required to improve the electrochemical properties significantly. An initial capacity of 500 mA h g^{-1} and a progressive capacity of $\sim 400 \text{ mA h g}^{-1}$ up to 100 cycles have been delivered by $\text{Li}_3\text{V}_2(\text{PO}_4)_3/\text{C}-20$ anode with an admissible capacity fade of 20 %, especially when cycled at a current density of 100 mA g^{-1} . The optimized $\text{Li}_3\text{V}_2(\text{PO}_4)_3/\text{C}-20$ composite thus demonstrates itself as a high capacity anode and finds its suitability for high rate applications by way of exhibiting appreciable capacity values of 450, 350, 302 and 220 mA h g^{-1} , under the influence of 100, 200, 300 and 400 mA g^{-1} current density.

1. INTRODUCTION

Lithium-ion batteries are the widely studied energy storage devices for application in portable electronic devices, electric vehicles (EV) and hybrid electric vehicles (HEV).¹⁻³ Considering an improvement with respect to power and energy density of lithium-ion batteries, selection of suitable electrodes gains importance. Graphite is the most widely used anode material, especially after the commercialization of Sony's lithium-ion battery in 2001. Driven by the low theoretical capacity and sloping voltage plateau of graphite,⁴ certain lithium alloying metal and tin oxides, viz., Mn_3O_4 ,⁵ Co_3O_4 ,⁶ SnO_2 ,⁷ CuO ,⁸ Fe_2O_3 ,⁹ and Fe_3O_4 ¹⁰ have been extensively studied along with the zero strain $\text{Li}_4\text{Ti}_5\text{O}_{12}$ anode.¹¹ However, issues such as larger irreversible capacity loss, volume expansion and higher intercalation potential of such anodes pose the necessity to identify and explore newer electrode materials as alternative anodes for lithium-ion batteries.

Transition metal phosphates as cathodes are popularly known for their high stability, rate capability and safety. On the other hand, Kalaiselvi et al.¹² in 2004 reported on the anodic behaviour of LiFePO_4 for lithium battery applications and LiVOPO_4 is another cathode material reported recently for its application as anode material.¹³

Towards this direction, monoclinic $\text{Li}_3\text{V}_2(\text{PO}_4)_3/\text{C}$, an upcoming cathode bestowed with high energy density, rate capability and safety intrigues recent researchers to explore the possibility of exploiting the same as an anode. Such an idea gets validated from the possible existence of vanadium in at least three different oxidation states and its ability to undergo insertion and/or alloying reaction with lithium in a wide potential range of 0.05 - 4.8 V. In this regard, X. H. Rui et al.¹⁴ reported on the performance of $\text{Li}_3\text{V}_2(\text{PO}_4)_3/\text{C}$ anode in the potential range of 3.0–0.0 V to obtain a capacity of 203 mAh g^{-1} versus Li^+/Li and W. F. Mao et al. discussed on the possible existence of $\text{Li}_3\text{V}_2(\text{PO}_4)_3$ (cathode)|| $\text{Li}_3\text{V}_2(\text{PO}_4)_3$ (anode) assembly.¹⁵ Herein, the open structure of $\text{Li}_3\text{V}_2(\text{PO}_4)_3$ allows the easy entry/departure of lithium ions into/from the electrode without causing structural change.

Quite different from such scarcely available reports on $\text{Li}_3\text{V}_2(\text{PO}_4)_3$ anode, our present work that deals with the investigation of combustion synthesized $\text{Li}_3\text{V}_2(\text{PO}_4)_3/\text{C}$ as a high capacity and high rate anode material is first of its kind to report on the possibility of extracting a high specific capacity of $\sim 400 \text{ mA h g}^{-1}$ under 100 mA g^{-1} , wherein the suitability of $\text{Li}_3\text{V}_2(\text{PO}_4)_3/\text{C}$ anode for high rate (400 mA g^{-1}) applications has also been demonstrated. The synergistic effect of oxalic dihydrazide assisted combustion method (ODHAC) and the optimized addition of super P carbon (20 wt.%) is believed to be responsible for the excellent electrochemical properties of $\text{Li}_3\text{V}_2(\text{PO}_4)_3/\text{C}$ anode.

Central Electrochemical Research Institute, Karaikudi- 630 006,
Tamilnadu, India

*Email: kalaiselvicecri@gmail.com [N. KALAISELVI]

2. EXPERIMENTAL PROCEDURE

2.1 Material synthesis of $\text{Li}_3\text{V}_2(\text{PO}_4)_3/\text{C}$

$\text{Li}_3\text{V}_2(\text{PO}_4)_3/\text{C}$ was synthesized by solution assisted combustion (SAC) method using oxalic dihydrazide (ODH) and the details of ODHAC method are reported elsewhere [16]. $\text{Li}_3\text{V}_2(\text{PO}_4)_3$ thus obtained was treated with different composition (10, 20 and 30 wt.%) of super P carbon and ball milled for 5 h at 300 rpm. Subsequently, the mixture was heated in furnace at 700 °C for 2 h to ensure better adherence of carbon on the surface of $\text{Li}_3\text{V}_2(\text{PO}_4)_3$ compound. Carbon coated $\text{Li}_3\text{V}_2(\text{PO}_4)_3$ samples thus prepared were investigated further for their performance as anode in lithium-ion cell assembly.

2.2 Physical and electrochemical characterization

The structure and phase purity of synthesized compound were examined with Bruker D8 Advance X-ray diffraction (XRD) using Ni-filtered Cu K α radiation ($\lambda = 1.5406 \text{ \AA}$). Particle size, carbon coating and surface morphology of synthesized active material were investigated using Tecnai 20 G2 (FEI make) Transmission Electron Microscopy (TEM) and Gemini Field Emission Scanning Electron Microscopy (FESEM). TG/DTA studies were performed using TA Instruments SDT Q600 thermogravimetric analyzer. Cyclic voltammetry (CV) was carried out using VMP3 multichannel potentiostat-galvanostat system (Biologic Science Instrument). Charge-discharge studies were carried out using ARBIN charge-discharge cyclers.

2.3 Electrode preparation and coin cell fabrication

Electrochemical characterization was carried out using CR2032 coin cells. Preparation of electrode and fabrication of coin cells are similar to our earlier reports¹² and the fabricated cells were subjected to charge-discharge studies galvanostatically in the voltage range of 3.0-0.05 V versus Li^+/Li at room temperature. Cyclic voltammetry (CV) measurements were performed at a scan rate of 0.2 mV s^{-1} between 0.05 and 3.5 V for the cells containing $\text{Li}_3\text{V}_2(\text{PO}_4)_3/\text{C}$ anode vs. Li metal separated by Celgard separator soaked in the electrolyte consisting of 1 M LiPF_6 dissolved in EC: DMC (1:1 v/v).

3. RESULTS AND DISCUSSION

3.1 Structural characterization - X-Ray Diffraction, TEM, FE-SEM and Elemental mapping

Fig.1 shows the XRD pattern of $\text{Li}_3\text{V}_2(\text{PO}_4)_3$ synthesized at 850 °C. The position and intensity of all peaks indicate the formation of polycrystalline $\text{Li}_3\text{V}_2(\text{PO}_4)_3$ with a monoclinic structure and P21/n space group. Indexing of miller indices (hkl) of respective diffraction peaks of $\text{Li}_3\text{V}_2(\text{PO}_4)_3$ evidences the absence of impurity peaks. The calculated lattice parameter values, viz., $a = 8.59 \text{ \AA}$, $b = 8.57 \text{ \AA}$, $c = 12.02 \text{ \AA}$ and $\beta = 90.5^\circ$ are in agreement with the literature report.¹⁷ Hence, it is understood that ODHAC method produces $\text{Li}_3\text{V}_2(\text{PO}_4)_3$ compound with desired purity and crystallinity. Particle size, and the presence of carbon on $\text{Li}_3\text{V}_2(\text{PO}_4)_3/\text{C}$ have been investigated by TEM studies (Fig.2) and the corresponding SAED pattern is appended as Inset of Fig. 2a. TEM image shows the presence of particles of ~100 nm size (Fig.2a). Further, TEM evidences the presence of carbon coating on $\text{Li}_3\text{V}_2(\text{PO}_4)_3$ particles (Fig.2b) and the thickness of such a continuous carbon coating is 15 nm

(Fig. 2c). SAED pattern (Inset of Fig. 2a) confirms the polycrystalline nature of pristine $\text{Li}_3\text{V}_2(\text{PO}_4)_3$ product, obtained from ODHAC method. Further, SAED pattern recorded for the carbon present in $\text{Li}_3\text{V}_2(\text{PO}_4)_3/\text{C}$ composite evidences the amorphous nature of added super P carbon (Fig. 2d)

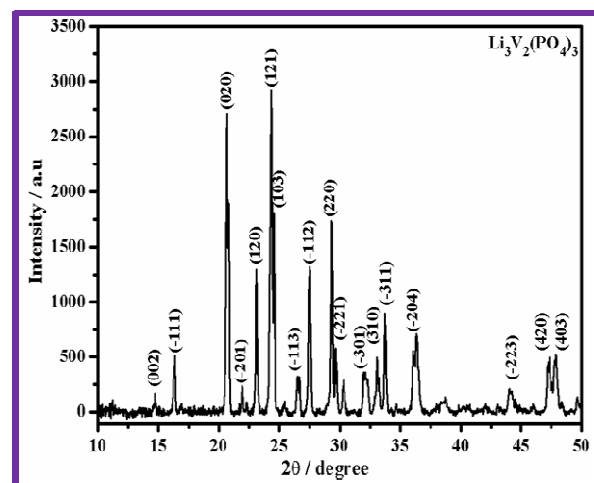


Fig. 1 XRD pattern of combustion synthesized $\text{Li}_3\text{V}_2(\text{PO}_4)_3$

The presence of carbon layer effectively suppresses the growth of $\text{Li}_3\text{V}_2(\text{PO}_4)_3$ particles during high calcination process and the carbon layer is expected to improve the electronic conductivity of pristine $\text{Li}_3\text{V}_2(\text{PO}_4)_3$, which is of great importance to improve the electrochemical properties. Further, the flaky appearance of combustion synthesised $\text{Li}_3\text{V}_2(\text{PO}_4)_3$ compound and the stoichiometry of $\text{Li}_3\text{V}_2(\text{PO}_4)_3/\text{C}$ composite are confirmed from FE-SEM and EDX analysis respectively.

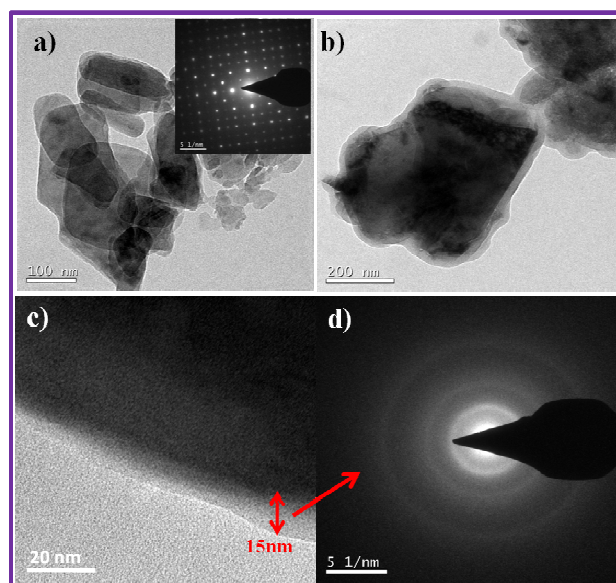


Fig. 2 a) Typical TEM image recorded for $\text{Li}_3\text{V}_2(\text{PO}_4)_3/\text{C}$ composite; Inset: SAED pattern of pristine $\text{Li}_3\text{V}_2(\text{PO}_4)_3$ and b) Presence of carbon coating on the surface of $\text{Li}_3\text{V}_2(\text{PO}_4)_3/\text{C}$ particles c) Figure showing the thickness of carbon coating d) SAED pattern evidencing the amorphous nature of super P carbon

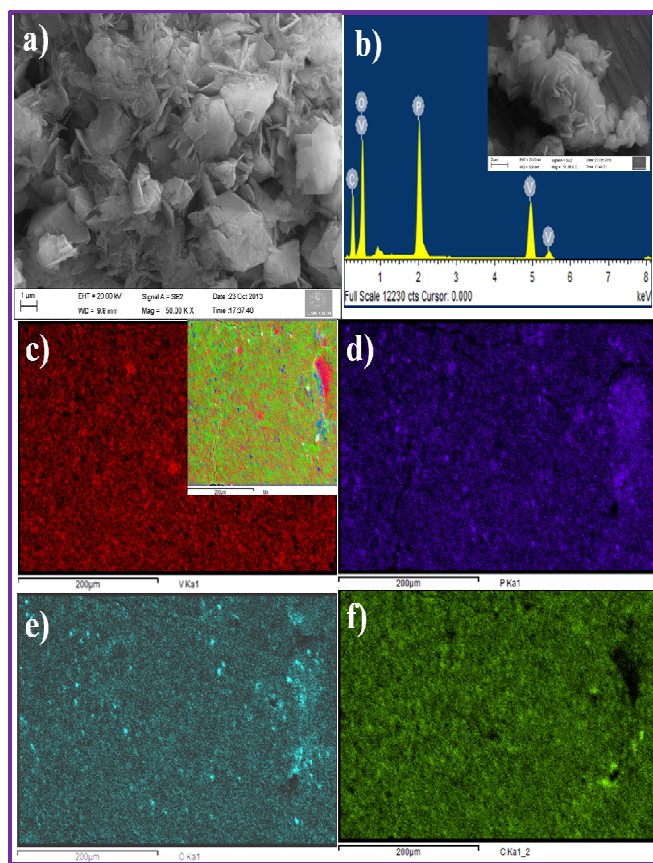


Fig. 3 a) FE-SEM image and b) EDX spectra recorded for $\text{Li}_3\text{V}_2(\text{PO}_4)_3/\text{C}-20$ composite; Inset: Closer view of flaky morphology; c-f) Elemental mapping of $\text{Li}_3\text{V}_2(\text{PO}_4)_3/\text{C}-20$ composite as a function of V,P,O and C contents individually Inset of 3c: Cumulative elemental mapping of $\text{Li}_3\text{V}_2(\text{PO}_4)_3/\text{C}-20$ composite

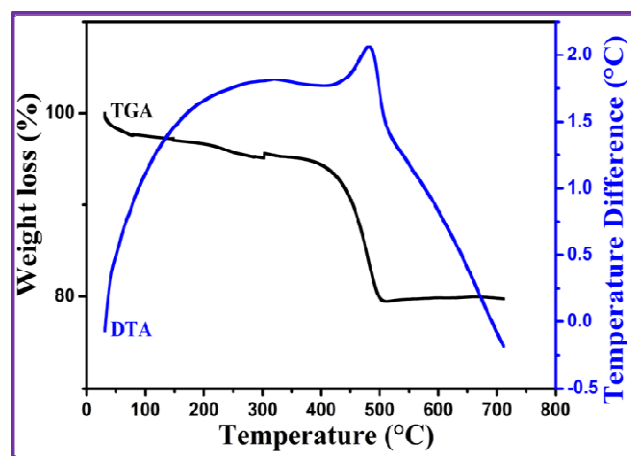


Fig. 4 TG/DTA results of $\text{Li}_3\text{V}_2(\text{PO}_4)_3/\text{C}-20$ composite

3.2 Cyclic Voltammetry studies

(Fig. 3a and b). Elemental mapping (Fig.3c-f) of $\text{Li}_3\text{V}_2(\text{PO}_4)_3/\text{C}$ composite, with a special reference to cumulative elemental mapping (Inset of Fig. 3c) confirms the presence of V, P, O and C in the individual particles. The total carbon content of the

title composite has been calculated using TG/DTA and is found to be 20 wt. % (Fig. 4)

Typical cyclic voltammetry (CV) behaviour of $\text{Li}_3\text{V}_2(\text{PO}_4)_3/\text{C}$ composite anode is shown in Fig.5. First cycle CV is quite different from the following cycles due to the formation of SEI

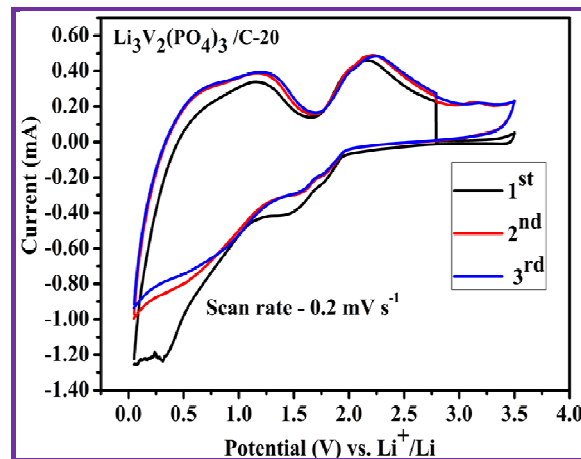


Fig. 5 Cyclic Voltammogram of $\text{Li}_3\text{V}_2(\text{PO}_4)_3/\text{C}-20$ anode

layer and is not unusual. Insertion/de-insertion of lithium occurs at different voltages, viz., 1.95/1.72, 1.86/1.77, 1.74/1.90, 1.65/2.02 V, corresponding to the formation of two phase ($>1.6\text{V}$) and single phase ($\leq 1.6\text{V}$) lithium insertion related intermediate compounds with varying lithium content,¹⁴ which is evident from CV cycles. However, a slight shift in peak position of first and successive CV curves is observed, which is due to the SEI formation driven unavoidable irreversible capacity loss with respect to the initial cycle. Interestingly, the following 2nd and 3rd cycles also show the presence of four red-ox pairs in the respective anodic region, thus confirming the reversibility and structural stability of currently synthesized $\text{Li}_3\text{V}_2(\text{PO}_4)_3/\text{C}$ anode.

3.3 Charge-discharge studies

Charge-discharge behaviour of $\text{Li}_3\text{V}_2(\text{PO}_4)_3/\text{C}$ anode consisting of 10, 20 and 30 wt.% of super P carbon under a current density of 100 mA g^{-1} is shown in Fig.6. The initial charge capacity

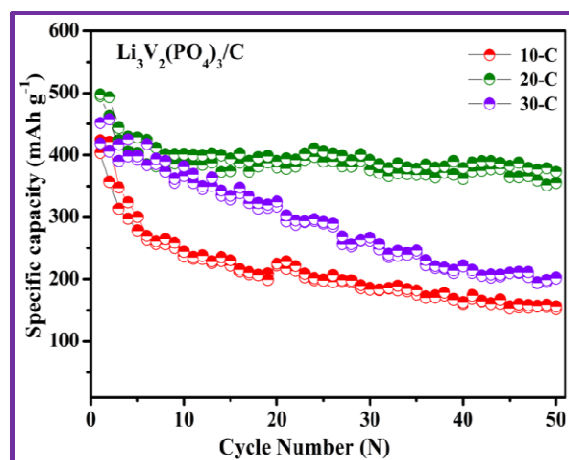


Fig. 6 Cycling behavior of $\text{Li}_3\text{V}_2(\text{PO}_4)_3/\text{C}$ anode with different carbon content (10, 20 and 30 wt.%)

corresponding to $\text{Li}_3\text{V}_2(\text{PO}_4)_3/\text{C}$ composite containing 10, 20 and 30 wt.% of carbon is found to be 414, 500 and 418 mA h g^{-1} . After 50 cycles, nominal specific capacity of 156, 400 and 201 mA h g^{-1} with a respective capacity retention of 38, 80 and 48 % has been exhibited by $\text{Li}_3\text{V}_2(\text{PO}_4)_3/\text{C}$ anode containing 10, 20 and 30 wt.% of carbon. From this observation, it is understood that 20 wt.% of super P carbon exhibits better cycling performance compared with those of 10 and 30 wt.% of super P carbon.

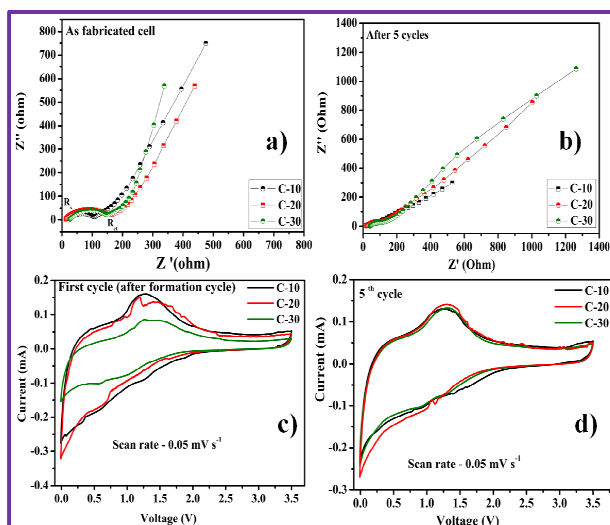


Fig. 7 Impedance spectra (a-b) and Cyclic voltammety (c-d) of $\text{Li}_3\text{V}_2(\text{PO}_4)_3/\text{C}$ composite anodes containing 10, 20 and 30 wt.% carbon

Even though it appears to be straight forward that an increasing carbon content would improve the electrochemical behaviour in a linear manner, the observed improvement in the electrochemical performance is not linear with the increasing carbon content.

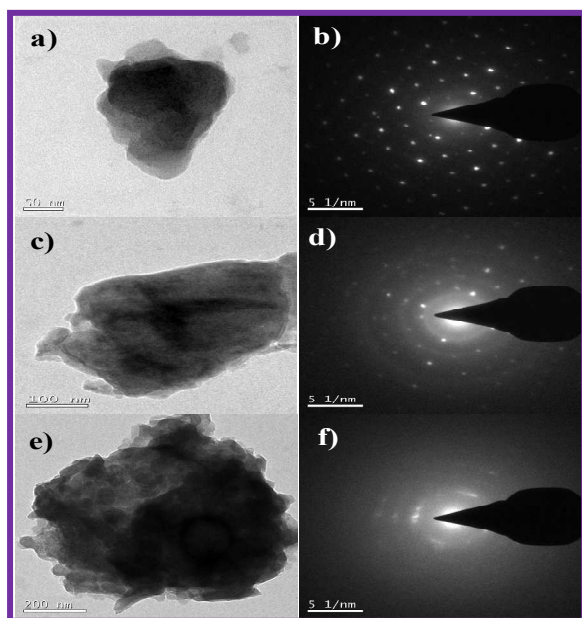


Fig. 8 TEM images and SAED pattern of $\text{Li}_3\text{V}_2(\text{PO}_4)_3/\text{C}$ composite containing (a-b) 10 (c-d) 20 and (e-f) 30 wt.% super P carbon.

Probable reason may be understood as follows: It is evident from figure 7 that the R_{ct} value of $\text{Li}_3\text{V}_2(\text{PO}_4)_3/\text{C}-20$ is lower than those of $\text{Li}_3\text{V}_2(\text{PO}_4)_3/\text{C}-10$ and $\text{Li}_3\text{V}_2(\text{PO}_4)_3/\text{C}-30$ anodes, especially upon cycling. Similarly, a higher peak current (i_p) has been exhibited upon cycling by $\text{Li}_3\text{V}_2(\text{PO}_4)_3/\text{C}-20$ anode in comparison with $\text{Li}_3\text{V}_2(\text{PO}_4)_3/\text{C}-10$ and $\text{Li}_3\text{V}_2(\text{PO}_4)_3/\text{C}-30$ anodes, thus substantiating the advantageous role of 20 wt.% carbon in improving the electrochemical behaviour of $\text{Li}_3\text{V}_2(\text{PO}_4)_3/\text{C}$ anode, by offering a desired conducting network to facilitate faster lithium diffusion kinetics.

In addition, the gradually reducing diffraction spots (Fig.8) observed in the SAED pattern with the increasing carbon content clearly evidences the fact that the intensity of carbon cloud is adversely high in $\text{Li}_3\text{V}_2(\text{PO}_4)_3/\text{C}-30$ composite to impede the faster diffusion of lithium ions. As a result, $\text{Li}_3\text{V}_2(\text{PO}_4)_3/\text{C}-20$ exhibits better electrochemical performance compared with those of $\text{Li}_3\text{V}_2(\text{PO}_4)_3/\text{C}-10$ and $\text{Li}_3\text{V}_2(\text{PO}_4)_3/\text{C}-30$ anodes.

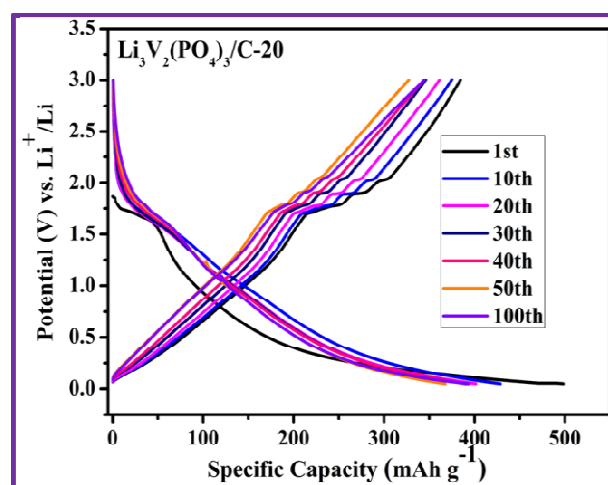


Fig. 9 Capacity vs. voltage profile of $\text{Li}_3\text{V}_2(\text{PO}_4)_3/\text{C}-20$ anode (100 mA g^{-1} current density)

Based on the above mentioned reasons, further studies such as extended charge-discharge studies and rate capability test were restricted to $\text{Li}_3\text{V}_2(\text{PO}_4)_3/\text{C}$ containing 20 wt.% carbon. The voltage profile of $\text{Li}_3\text{V}_2(\text{PO}_4)_3/\text{C}-20$ anode corresponding to 1, 10, 20, 30, 40, 50 and 100 cycles are shown in Fig.9, wherein consistent appearance of voltage plateaus at the respective positions is observed up to 100 cycles, with an exception of initial discharge curve. The appreciable capacity retention and the admissible fade ($\sim 20\%$) in capacity of $\text{Li}_3\text{V}_2(\text{PO}_4)_3/\text{C}-20$ anode, as evident from Fig.10 are in favour of considering the same as a potential anode for lithium battery applications. In other words, a reasonable capacity of 400 mA h g^{-1} that has been observed up to 100 cycles under the influence of 100 mA g^{-1} current density substantiates the superiority of currently synthesized $\text{Li}_3\text{V}_2(\text{PO}_4)_3/\text{C}-20$ anode over conventional graphite.

In addition, the currently observed capacity of 400 mA h g^{-1} under the influence of 100 mA g^{-1} current density is found to be superior than the capacity value reported for $\text{Li}_3\text{V}_2(\text{PO}_4)_3/\text{C}$ anode and the irreversible capacity loss of 20 mA h g^{-1} is also nominal compared with the literature report.¹⁴

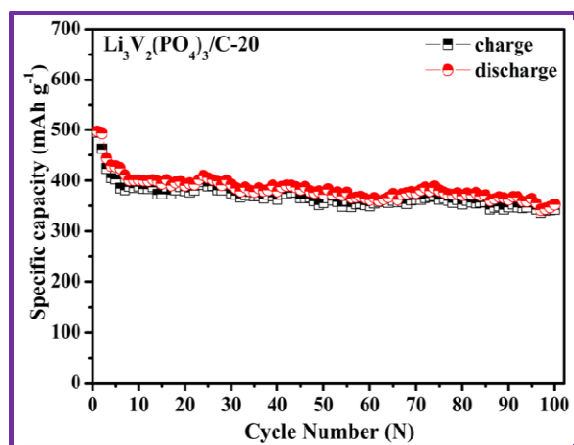


Fig. 10 Charge–discharge behavior of $\text{Li}_3\text{V}_2(\text{PO}_4)_3/\text{C}-20$ anode upon extended cycling (100 mA g^{-1} current density)

Hence, it is understood that the amount of carbon plays a crucial role in deciding the electrochemical performance and the 20 wt.% carbon has been identified as the optimum concentration to prepare $\text{Li}_3\text{V}_2(\text{PO}_4)_3/\text{C}$ anode with appreciable specific capacity behaviour.

3.4 Rate Capability Test

The rate capability behavior of $\text{Li}_3\text{V}_2(\text{PO}_4)_3/\text{C}-20$ anode was investigated upon progressive cycling as a function of different current densities such as 100, 200, 300 and 400 mA g^{-1} (Fig. 11).

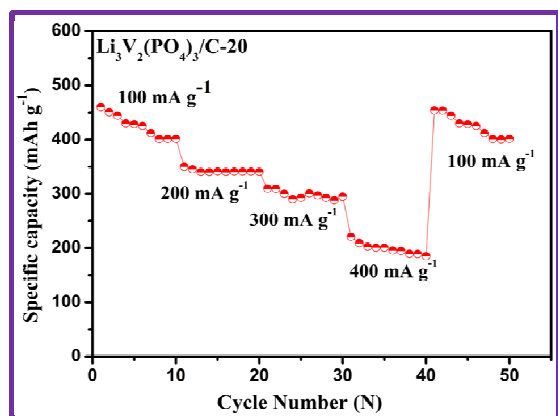


Fig. 11 Rate capability behaviour of ODHAC synthesized $\text{Li}_3\text{V}_2(\text{PO}_4)_3/\text{C}-20$ anode

$\text{Li}_3\text{V}_2(\text{PO}_4)_3/\text{C}-20$ anode exhibits acceptable capacity values of 450, 350, 302 and 220 mA h g^{-1} corresponding to a current density of 100, 200, 300 and 400 mA g^{-1} respectively. Interestingly, $\text{Li}_3\text{V}_2(\text{PO}_4)_3/\text{C}-20$ anode is found to resume the initial capacity of $\sim 400 \text{ mAh g}^{-1}$ even after subjecting the same to higher current densities such as 200, 300 and 400 mA g^{-1} , which is in favour of the suitability and structural stability of the same for high rate applications.

Conclusions

ODHAC method, by virtue of offering phase pure $\text{Li}_3\text{V}_2(\text{PO}_4)_3$ compound and its synergy with the addition of optimized

amount of 20 wt.% of super P carbon results in the formation of $\text{Li}_3\text{V}_2(\text{PO}_4)_3/\text{C}-20$ anode, which in turn is responsible for the improved electrochemical behaviour. Accordingly, $\text{Li}_3\text{V}_2(\text{PO}_4)_3/\text{C}-20$ anode delivers an appreciable specific capacity of $\sim 400 \text{ mA h g}^{-1}$ up to 100 cycles under the influence of 100 mA g^{-1} current density. Inferior electrochemical properties observed with 10 and 30 wt.% super P carbon enunciates the crucial role of addition of 20 wt.% carbon in offering a desirable conducting network to facilitate facile lithium diffusion kinetics and to improve the electrochemical behaviour. The study recommends the suitability of high capacity $\text{Li}_3\text{V}_2(\text{PO}_4)_3/\text{C}-20$ anode for high rate applications, as evident from the extraction of nominal capacity of $\sim 220 \text{ mA h g}^{-1}$ under 400 mA g^{-1} condition.

Acknowledgements

Among the authors, V. Mani is thankful to DST, New Delhi and K. Nathiya to CSIR, New Delhi for financial support through CSIR-EMPOWER Project. N. Kalaiselvi is thankful to CSIR, New Delhi and DST, New Delhi for support through CSIR-EMPOWER and Grant-in-aid Project (GAP) respectively.

Notes and references

- 1 Citations here in the format 1 J. Goodenough, Y. Kim, Chem. Mater., 2010, **22**, 587-603.
- 2 J. M. Tarascon, M. Armand, Nature, 2001, **414**, 359-367.
- 3 C. M. Park, J. H. Kim, H. Kim and H. J. Sohn, Chem. Soc. Rev., 2010, **39**, 3115-3141.
- 4 H. Nozakia, K. Nagaokab, K. Hoshib, N. Ohtaa, M. Inagaki, J. Power Sources, 2009, **194**, 486-493.
- 5 H. Wang, L. F. Cui, Y. Yang, H. S. Casalongue, J. T. Robinson, Y. Liang, Y. Cui, H. Dai, J. Am. Chem. Soc., 2010, **132**, 13978-13980.
- 6 Y. M. Kang, M. S. Song, J. H. Kim, H. S. Kim, M. S. Park, J. Y. Lee, H. K. Liu, S. X. Dou, Electrochim. Acta, 2005, **50**, 3667-3673.
- 7 N. Li, C. R. Martin, B. Scrosati, Electrochem. Solid State Lett. 2000, **3**, 316-318.
- 8 J. Y. Xiang, J. P. Tu, L. Zhang, Y. Zhou, X. L. Wang, S. J. Shi, J. Power Sources, 2010, **195**, 313-319.
- 9 H. Liu, G. Wang, J. Park, J. Wang, H. Liu, C. Zhang, Electrochim. Acta, 2009, **54**, 1733-1736.
- 10 S. Ito, K. Nakaoka, M. Kawamura, K. Ui, K. Fujimoto, N. Koura, J. Power Sources, 2005, **146**, 319-322.
- 11 L. Aldon, P. Kubiak, M. Womes, J. C. Jumas, J. O. Fourcade, J. L. Tirado, J. I. Corredor, C. P. Vicente, Chem. Mater., 2004, **16**, 5721-5725.
- 12 N. Kalaiselvi, C. H. Doh, C. W. Park, S. I. Moon, M. S. Yun, Electrochem. Commun., 2004, **6**, 1110-1113.
- 13 M. M. Ren, Z. Zhou, X. P. Gao, J. App. Electrochem., 2010, **40**, 209-213.
- 14 X. H. Rui, N. Yesibolati, C. H. Chen, J. Power Sources, 2011, **196**, 2279-2282.
- 15 W-F Mao, H-Q Tang, Z-Y Tang, J. Yan, Q. Xu, ECS Electrochem. Lett., 2013, **2** (7), A69-A71.
- 16 K. Nathiya, D. Bhuvanewari, Gangulibabu, D. Nirmala, N. Kalaiselvi, RSC Advances, 2012, **2**, 6885-6889.
- 17 Y. Li, L. Honga, J. Suna, F. Wua, S. Chen, Electrochim. Acta, 2012, **85**, 110-115.